JOURNAL OF VIROLOGY, Dec. 2007, p. 13761–13770 Vol. 81, No. 24
0022-538X/07/$08.00+0 doi:10.1128/JVI.01290-07

Discrete Clusters of Virus-Encoded MicroRNAs Are Associated with Complementary Strands of the Genome and the 7.2-Kilobase Stable Intron in Murine Cytomegalovirus▽

Amy H. Buck,[1]* Javier Santoyo-Lopez,[1] Kevin A. Robertson,[1] Diwakar S. Kumar,[1] Martin Reczko,[2] and Peter Ghazal[1]

Division of Pathway Medicine, University of Edinburgh, Edinburgh, United Kingdom,[1] and Foundation for Research and Technology—Hellas (FORTH), Heraklion, Greece[2]

Received 13 June 2007/Accepted 1 October 2007

The prevalence and importance of microRNAs (miRNAs) in viral infection are increasingly relevant. Eleven miRNAs were previously identified in human cytomegalovirus (HCMV); however, miRNA content in murine CMV (MCMV), which serves as an important in vivo model for CMV infection, has not previously been examined. We have cloned and characterized 17 novel miRNAs that originate from at least 12 precursor miRNAs in MCMV and are not homologous to HCMV miRNAs. In parallel, we applied a computational analysis, using a support vector machine approach, to identify potential precursor miRNAs in MCMV. Four of the top 10 predicted precursor sequences were cloned in this study, and the combination of computational and cloning analysis demonstrates that MCMV has the capacity to encode miRNAs clustered throughout the genome. On the basis of drug sensitivity experiments for resolving the kinetic class of expression, we show that the MCMV miRNAs are both early and late gene products. Notably, the MCMV miRNAs occur on complementary strands of the genome in specific regions, a feature which has not previously been observed for viral miRNAs. One cluster of miRNAs occurs in close proximity to the 5′ splice site of the previously identified 7.2-kb stable intron, implying a variety of potential regulatory mechanisms for MCMV miRNAs.

Small noncoding RNAs (ncRNAs) play diverse roles in biological pathways and are increasingly prevalent in the viral context (37, 48). One particular class of ncRNAs, microRNAs (miRNAs), regulates eukaryotic gene expression by binding to specific mRNA transcripts and initiating their degradation or repressing their translation (22, 24, 26). Despite the relatively recent discovery of miRNAs in *Caenorhabditis elegans*, research in this field has progressed rapidly in a number of species, and it is now estimated that miRNAs comprise 1% of genes in animals and may target up to 30% of genes in humans (28). This highly significant class of molecules, therefore, has an enormous capacity to modulate the transcriptome, and it is not surprising that viruses have found a way to exploit this regulatory system. Given their small size (~22 nucleotides [nt]) and their large potential for gene regulation (multiple targets), miRNAs offer a particularly efficient mechanism for viruses to manipulate viral and cellular pathways. First discovered in Epstein-Barr virus (EBV) in 2004 (38), viral miRNAs have now been characterized in the three herpesvirus subfamilies (36) and in polyomaviruses (49) and adenoviruses (30, 43). Reports have also emerged detailing miRNA discovery in retroviruses (3, 35).

In the realm of virus-host interactions, miRNAs have been shown to function in a variety of capacities (33, 44, 45). Viral miRNAs can target viral genes, most obviously when the target is encoded on the opposite strand from the miRNA, as implicated in EBV (10, 38) and demonstrated in simian virus 40 (SV40). In SV40, this can serve in immune evasion, since SV40 miR-S1 targets the viral large T antigen at late stages of infection and protects cells from being killed by cytotoxic T lymphocytes (49). There are also examples of host miRNAs serving proviral or antiviral functions. Specifically, human mir-32 has an antiviral effect on primate foamy virus 1, since it targets viral mRNA in kidney cells and inhibits primate foamy virus replication (25). In contrast, mir-122, a liver-specific host miRNA, has a proviral effect in hepatitis C virus by interacting with the 5′ noncoding region of the viral genome and increasing its expression (18). Recent reports with herpes simplex virus type 1 (HSV-1) and human cytomegalovirus (HCMV) have demonstrated that virus-encoded miRNAs can also target specific cellular genes involved in apoptosis and host immune defense. In HSV-1, the virus-encoded mir-LAT down regulates two proteins (TFGB and SMAD3) which induce apoptosis in infected cells (16) and thereby contributes to the ability of the virus to persist in a latent form. In the case of HCMV, mir-UL112 targets the major histocompatibility complex class I-related chain B gene, whose absence protects HCMV-infected cells from lysis by natural killer cells (47).

The majority of published viral miRNAs have been found in the herpesvirus family (36). There are several reasons which may explain this. First, double-stranded DNA viruses that replicate in the nucleus are the most likely candidates to utilize the host miRNA machinery as well as RNA polymerase II, from which most miRNAs derive (27). Second, since the prototypic effect of a miRNA is the reduction of target protein production, it has been hypothesized that viruses with longer life cycles or those capable of latent infection (a characteristic of herpesviruses) are more likely to utilize this regulatory mechanism (6). This hypothesis relates to the assumption that a pool

* Corresponding author. Mailing address: Division of Pathway Medicine, University of Edinburgh, Edinburgh, United Kingdom. Phone: 44 131 242 6280. Fax: 44 131 242 6244. E-mail: a.buck@ed.ac.uk.

▽ Published ahead of print on 10 October 2007.

of target protein must decay before any virus-specific effect can be observed. It is highly relevant, therefore, to study the function and mechanisms of miRNA action in herpesvirus systems which have well-established models for infection and pathogenesis.

Of particular interest in this regard is HCMV, a member of the betaherpesvirus family which infects 50 to 90% of the world's population and is the most common infectious agent transmitted via blood transfusion (14). Previous work has shown that HCMV encodes at least 11 miRNAs (7, 13, 36), and one of these miRNAs has been shown to target a host immune system gene (cited above). CMV is highly species specific; however, the pathogenesis of mouse CMV (MCMV) in mice is remarkably similar to that of HCMV in humans. This has resulted in the widespread adoption of the MCMV model in the study of all aspects of infection and pathogenesis (19).

In the present study, we examine the presence of miRNAs in MCMV using both computational and RNA cloning approaches. This is the first report of miRNAs in MCMV and should stimulate further work regarding the function of these molecules in infection.

MATERIALS AND METHODS

MicroRNA prediction analysis. Precursor feature classification using support vector machines (SVM) was employed to predict the locations of MCMV miRNA precursor stem-loop structures. Our procedure implemented the following steps. (i) Both strands of the MCMV genome (230,278 bp) were scanned using a sliding window of 104 nt, and RNA secondary structure was predicted using the RNAfold program (17). (ii) For stable structures with a minimum free energy of less than −15 kcal/mol, a total of seven structural and energetic features were extracted and classified using a SVM trained on known positive and negative miRNA examples. Using a probability model (40), the SVM generates a score for each hairpin ranging from 0 to 1.3. As there is evidence that miRNA precursors, unlike other ncRNAs, have lower folding free energies than random sequences, this property was assessed using the RANDfold program (4).

Cells and viruses. Primary mouse embryonic fibroblasts (MEF) (prepared from BALB/c mice) and NIH 3T3 (ATCC CRL-1658) cells were maintained in Dulbecco's modified Eagle's medium (Invitrogen) supplemented with 10% fetal calf serum (10% calf serum for NIH 3T3 cells) and 1% penicillin-streptomycin as previously described (12). Bone marrow-derived macrophages (BMM) were obtained from femur cells of male mice 10 to 12 weeks after gestation using standard protocols; cells were maintained in Dulbecco's modified Eagle's medium-F12, with 10% L929-conditioned medium, 10% fetal calf serum, and 1% penicillin-streptomycin. Cells were either mock infected or infected with wild-type virus (Smith strain) generated from the recombinant C3X bacterial artificial chromosome clone described in reference 11. Virus was propagated in NIH 3T3 cells, and titers were determined by standard plaque assay on MEF.

Cloning and sequencing. Small RNAs were cloned following a protocol similar to previously described protocols (24, 36). Briefly, BMM and MEF cells were infected with virus at a multiplicity of infection (MOI) of 1.0. RNA was extracted using TRIzol (Invitrogen) after 72 h, and 100 μg was loaded onto a 15% denaturing gel using radiolabeled RNA markers of 19 and 24 nt (CGUACGC GGGUUUAAACCA and CGUACGCGGAAUAGUUUAAACUGU) that contained PmeI restriction sites (36). The gel slice was eluted overnight in 0.1 mM EDTA and then ethanol precipitated. Purified RNA was ligated with T4 RNA ligase (New England Biolabs) to a 5′ adapter (ATCGTaggcaccugaaa [DNA shown in uppercase and RNA shown in lowercase]; Eurogentec) and a 5′ adenylated 3′ adapter available from Integrated DNA Technologies (rAppCTG TAGGCACCATCAAddC, which is used for MEF cloning, and rAppTTTAAC CGCGAATTCCAGddC, which is used for BMM cloning). Adapters were designed to prevent self-ligation, and products were gel purified after each step. Ligated RNA was reverse transcribed (ATTGATGGTGCCTAC) using Superscript III reverse transcriptase (Invitrogen) and PCR amplified (forward primer, ATCGTAGGCACCTGAAA; reverse primer, ATTGATGGTGCCTACAG). PCR products were digested with PmeI (to eliminate size markers) and BanI, followed by concatamerization with T4 DNA ligase (New England Biolabs). Concatemers were incubated with *Taq* DNA polymerase to fill in the 3′ ends and were then cloned (TOPO TA cloning kit; Invitrogen) and sequenced (GATC Biotech). The 392 sequenced clones from MEF and 212 clones from BMM were blasted against the mouse and viral genomes, allowing for two gaps or mismatches. After validation, the raw sequence data were reexamined for the viral clones to allow for additional mismatches (primarily additions of nongenomic sequence at the 3′ end, as reported below in Table 2).

Northern blot analysis. Northern blots were performed based on protocols described elsewhere (26) (web.wi.mit.edu/bartel/pub). Briefly, RNA was extracted from NIH 3T3 cells that were mock infected or infected with MCMV at a MOI of 2 after 72 h.

The integrity of the RNA was assessed according to the standards developed with the 2100 Bioanalyzer (Agilent); all RNA samples used for analysis had an RNA integrity number (RIN number) of >9.0, indicating high-quality RNA with minimal degradation products. Twenty micrograms of RNA per lane was loaded onto a 15% polyacrylamide gel, along with ^{32}P-labeled Decade RNA markers (Ambion) and then electroblotted onto a GeneScreen Plus membrane (Perkin-Elmer). Membranes were hybridized overnight with ^{32}P-labeled probes complementary to the mature miRNA. We also tested probes with locked nucleic acid substitutions at every third position for mir-M23-1, mir-m59-1-5p, mir-m59-2, and mir-m107-1-3p, which displayed a faint signal with the unmodified probes; these probes were hybridized and washed under low-stringency conditions as described elsewhere at 37 to 42°C (51). However, this did not significantly improve detection, and results are shown below in Fig. 2 are with unmodified probes, with the exception of mir-m59-2. Probes complementary to murine mir-16 and murine 5S RNA (AAGCCTACAGCACCCGGTATTC) were used as positive controls. Membranes were exposed to a PhosphorImager overnight, scanned with a Typhoon scanner, and imaged using ImageQuant (Molecular Dynamics); membranes were stripped and reused up to four times.

RT-PCR. RNA extracted for cloning studies (prior to size fractionation [see above]) was used for the reverse transcription-PCR (RT-PCR) experiments in Fig. 4 (infections were performed with NIH 3T3 cells, MEF, and BMM cells in parallel). For kinetic class experiments, NIH 3T3 cells were incubated with cycloheximide (Sigma) at 100 μg/ml for 30 min prior to infection (MOI of 2) until 24 h postinfection (2). Experiments were also performed in the presence or absence of phosphonoacetic acid (Sigma) at 250 μg/ml for 24 h. RNA samples were treated with DNase (Invitrogen) prior to reverse transcription (although DNase treatment did not alter quantitative RT-PCR [qRT-PCR] results compared to non-DNase-treated RNA [data not shown]). qRT-PCR was performed using the Ncode SYBR green miRNA qRT-PCR kit (Invitrogen). Briefly, the extracted total RNA was poly(A) tailed and then subjected to reverse transcription with a poly(T) adapter primer. qRT-PCR was then performed using the reverse qRT-PCR primer provided in the kit and a forward primer identical in sequence to the mature miRNA of interest (exceptions are noted below). In this protocol, the amplified product is roughly ~65 nt long and includes the mature miRNA sequence, a portion of the poly(A) tail, and the sequence incorporated by the poly(T) adapter primer. Data were collected using the Mx3000P instrument (Stratagene) and analyzed with the associated software. Conditions were optimized so that only one dissociation product was observed with each primer. This required using a temperature cycle of 50°C for 2 min, 95°C for 2 min, followed by 45 cycles (with 1 cycle consisting of 15 s at 95°C, 15 s at 64°C and 20 s at 72°C), as previously reported in detail (46). All miRNAs validated in this study (listed below in Table 2) were analyzed by qRT-PCR except for the sequences labeled with asterisks and mir-M95-1, mir-M23-2, and mir-m107-1-3p (probes against the latter two yielded a signal in samples in which Dicer was knocked down, which indicates that they are not specific for detection of the mature miRNA and were therefore excluded from analysis; A. Buck, unpublished data). All forward primers were identical to the miRNA sequences listed in Table 2 (unbracketed), with the following exceptions, which were shortened by 1 or 2 nt at the 3′ end: mir-m01-4, TCCTATGCTAACACGTGCGCG; mir-m22-1, TTC CCCGTCCGTACCGAGGC; mir-M88-1, CAGAAGTCGATGTCGGGGT; and mir-m108-2-3p, GTGACTCGAGACGAGTGACCG. Standard curves for all miRNA primers demonstrated between 95 and 110% PCR efficiency as well as homogeneous dissociation curves with the expected melting temperature (74 to 78°C) (46). A probe to detect murine 5S RNA was used for normalization of qRT-PCR data; the probe was designed to be identical to the 3′ end of murine 5S RNA (5′-GAATACCGGGTGCTGTAGGCTT-3′). RT-PCR products were examined on 2.5% agarose gels as well as Lab901 D800 ScreenTape, which automatically separated and sized the amplified products by gel electrophoresis and integrated software.

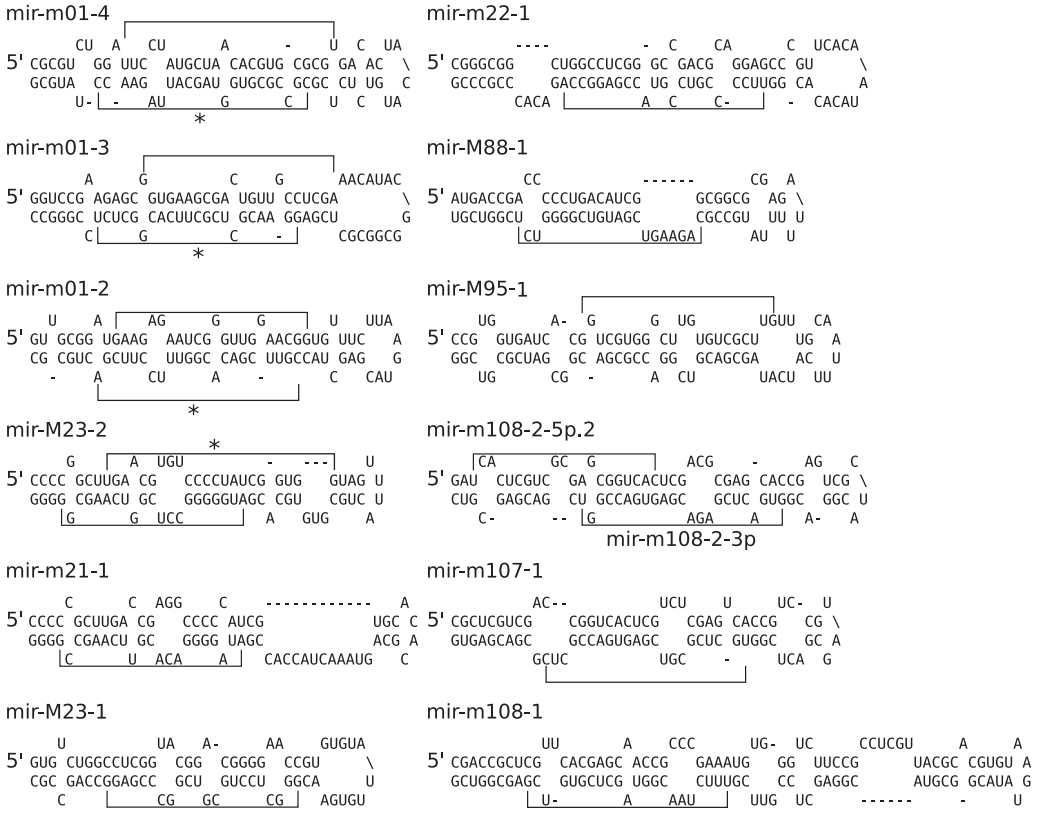

FIG. 1. Secondary structures of MCMV precursor miRNAs. The predicted stem-loop structures from the mfold program are depicted with cloned miRNAs indicated in brackets. Two mature miRNAs were cloned from the stem-loop precursors for mir-m01-4, mir-m01-3, mir-m01-2, and mir-M23-2; the asterisk indicates the sequence that is less likely to be incorporated into the RNA-induced silencing complex. We depict only one precursor for mir-m108-2-3p and mir-m108-2-5p.2, although the organization of these mature miRNAs within the precursor (5′ overhangs) is not characteristic of a typical intermediate.

RESULTS

Computational prediction of MCMV miRNAs. On the basis of the success of miRNA computational predictions in other herpesviruses (36), we applied precursor feature classification (using a machine learning approach) with support vector machines to classify the occurrence of precursor miRNAs in MCMV. A total of 105,051 hairpin structures predicted by the RNAfold program were classified by the SVM, and using a lower bound of 0.1 for the SVM score, 6,840 hairpins were subsequently processed by the RANDfold program. This program reshuffles the sequence and predicts corresponding structure for each of the hairpins based on 500 simulations. On the basis of permutation testing from the simulation runs, we assigned the reported *P* value to exceed 0.08 and obtained 2,155 hairpin structures (this cutoff has 95% sensitivity for known human miRNAs). After removing overlapping predictions, 582 remained.

Of the 12 precursor miRNAs cloned in this study (Fig. 1), 9 were represented in these predictions, representing 75% sensitivity. This method appears slightly more sensitive than another prediction method reported recently (where 7 of the 12 precursors cloned here were represented in the 579 predictions) (29). However, such a large number of predictions is not highly useful if the vast majority are false positives and the intent is to pursue target prediction or experimental validation. We therefore examined the specificity of our predictions by further ranking them according to the SVM score. The nine cloned and predicted precursors ranked throughout the top half of the list of 582 predicted hairpin structures (from number 3 to number 263); notably, 4 of the cloned precursors are represented in the top 10 predictions (listed in Table 1), and an

TABLE 1. Locations of predicted precursor miRNAs on the MCMV genome

SVM score	*P* value[a]	Location (nt)[b]
0.99997	0.00399	90262–90366 (−)
0.99996	0.00200	**131297–131401 (+)**
0.99993	0.00798	556–660 (+)
0.99991	0.00200	**23446–23550 (−)**
0.99990	0.01198	174754–174858 (−)
0.99989	0.00200	1985–2089 (−)[c]
0.99988	0.00200	**561–665 (−)**
0.99988	0.00200	57377–57481 (−)[c]
0.99971	0.00200	**23645–23749 (−)**
0.99970	0.00399	204375–204479 (+)

[a] *P* values from RANDfold program.

[b] The location of the predicted precursor miRNA on the plus strand (+) or minus strand (−) is indicated in parentheses. The precursors in bold type were validated in this report.

[c] These precursors were validated in the accompanying report by Dölken et al. (6a).

TABLE 2. MCMV miRNAs isolated from MEFs

MCMV miRNA[a]	Sequence[b]	No. of clones	Genome location (nt)[c]
mir-m01-4*	CGCCGCGUGGUAGCAUUAGAACC	2	394–416 (−)
mir-m01-4	UCCUAUGCUAACACGUGCGCGU[GA]	4	435–456 (−)
mir-m01-3*	GGAACGCUCGCUUCACGGCUCU	1	574–595 (−)
mir-m01-3	GGUGAAGCGACUGUUGCCUCGA[A]	38	615–636 (−)
mir-m01-2*	CGUUCGACACGGUUUCCUUCGA	4	770–791 (−)
mir-m01-2	GAAGAGAAUCGGGUUGGAACGG[U]	2	813–834 (−)
mir-M23-2[d]	AUGGGGGCCUCGGUCAAGCGG[(UAC)]	5	23468–23488 (−)
	CACGAUGGGGGCCUCGGUCAAG	1	23471–23492 (−)
mir-M23-2*	UGAACGUGUCCCCUAUCGGUGG	2	23509–23530 (−)
mir-m21-1	AUAGGGGACACGUUCAAGCCG	1	23515–23535 (+)
mir-M23-1	GGGCUCCUGCGUCGGCCCGAGG[C(U)A]	3	23668–23689 (−)
mir-m22-1	UUCCCCGUCCGUACCGAGGCCA[(AU)]	2	23707–23728 (+)
mir-M88-1	CAGAAGUCGAUGUCGGGGUCU	5	131357–131377 (+)
mir-M95-1	GGUCGUGGGCUUGUGUCGCUUG[(A)]	3	138206–138226 (+)
mir-m108-2-3p	GUGACUCGAGACGAGUGACCGGU[C(A)]	24	162073–162095 (−)
mir-m108-2-5p.2	UCACUCGUCGCGAGCGGUCAC[(C)]	4	162125–162145 (−)
mir-m107-1-3p	UGCUCGCGUCGAGUGACCGCUC	1	162113–162134 (+)
mir-m108-1[e]	UUUCUGACGGUGGCUCGUGUCG	2	162364–162385 (−)
mir-m55-1[f]	UGGUGAUCGGCGUGCUAGCCGUCGU	3	83412–83436 (−)
mir-m59-1(5p)[d,f]	CGCUGUCGGCCGAGGCACUGC	1	94485–94505 (+)
	GCUGUCGGCCGAGGCACUGCU	3	94486–94506 (+)
	UGUCGGCCGAGGCACTGCUCCU	1	94488–94509 (+)
mir-m59-2[f]	CCGAAGAGCCCUCACAGAGCC	4	94970–94990 (+)
mir-M87-1[f]	AGGCAGCCGUCGGCAGCGGCAG(AGA)	2	128875–128896 (+)

[a] The MCMV miRNA names listed in bold type are miRNAs whose precursors were predicted by computational analysis. An asterisk at the end of the miRNA name indicates that it is less likely to be incorporated into the RNA-induced silencing complex.

[b] The nucleotides noted in brackets represent additional nucleotides that were sequenced in a minority of the clones. Nucleotides in parentheses are not consistent with the genomic sequence (if they were cloned multiple times, the most common nucleotide is listed).

[c] The location of the predicted precursor miRNA on the plus strand (+) or minus strand (−) is indicated in parentheses.

[d] The cloned sequence variations of the RNAs are listed to depict the 5′ heterogeneity; mir-m59-1 is listed as "5p," since the other arm of the precursor was cloned by Dölken et al. (6a).

[e] The nucleotides underlined in the mir-m108-1 sequence are listed as adenosines in GenBank (NC_004065); sequencing of our recombinant virus, as well as the Smith strain virus from the ATCC, revealed that the nucleotides in the genomic sequence at these positions are guanosines (data not shown).

[f] These were not scored as miRNAs in this report but are named according to the accompanying report by Dölken et al. (6a).

additional 2 were validated in the accompanying report by Dölken et al. (6a), giving a success rate of 6/10 for this cutoff. This demonstrates that the SVM score (derived as described above) is a useful criterion for scoring miRNAs; additional analysis, such as deep sequencing, may shed light on how to better refine the best cutoff for specificity. It is worth mentioning that in this list of 10 precursors, two of the predictions are the reverse complements of one another (nt 556 to 660 on the plus strand and nt 561 to 665 on the minus strand [Table 1]), such that stem-loop structures are predicted on complementary strands of genome in specific locations. This is consistent with our cloning results that demonstrate miRNAs are derived from complementary strands of the genome in overlapping regions (below).

Sequencing results of miRNAs cloned from infected cells. Cloning of small RNAs has proven a successful method for experimentally identifying miRNAs in a variety of viruses (36). In two previous cloning studies with HCMV, either ~1% or ~18% of the total clones in each study possessed viral content, potentially due to differences in the infection conditions or cell lines (7, 36). Thus, in order to screen for an efficient experimental design in our cloning studies, we initially sequenced a set of clones (~200 each) from both infected MEF and BMM cells after 72 h. The ratio of viral to mouse RNA was assessed by BLAST analysis and was substantially greater in the MEF cells than in the BMM cells (~30% viral clones compared to 0.5% viral clones, respectively). We therefore performed additional sequencing with the infected MEF cells to isolate 123 viral clones (31% of the 392 total clones). From these clones, a total of 24 unique small viral RNAs were identified, and 17 of these sequences were scored as miRNAs according to the following criteria. (i) The sequence flanking the miRNAs is predicted to fold into a stem-loop structure with the lowest free energy. (ii) The cloned sequence is detected as a homogeneous band of the appropriate size on a Northern blot (1). In four cases, two of the cloned miRNAs originated from the same precursor (noted in Table 2). We have used asterisks to indicate the strand that is less likely to be incorporated into the RNA-induced silencing complex, according to the higher stability of base pairing at the 5′ end, although it appears likely that both strands could function as miRNAs, since they are readily detected by Northern blot analysis (Fig. 2A). Four additional cloned RNAs were detected by Northern blotting (listed in Table 2), but we did not classify these as miRNAs based on their faint and heterogeneous detection (mir-m59-1-5p, mir-m59-2, and mir-M87-1) or length (mir-m55-1, cloned as 25 nt). However, we have named them to be consistent with the accompanying report by Dölken et al. (6a), in which the RNAs were scored as miRNAs (mir-m59-1-5p is in the 5′ arm of the depicted pre-miRNA for mir-m59-1 in that study). A distinction between our two studies is that we utilized Northern blot detection as a criterion for scoring miRNAs. However,

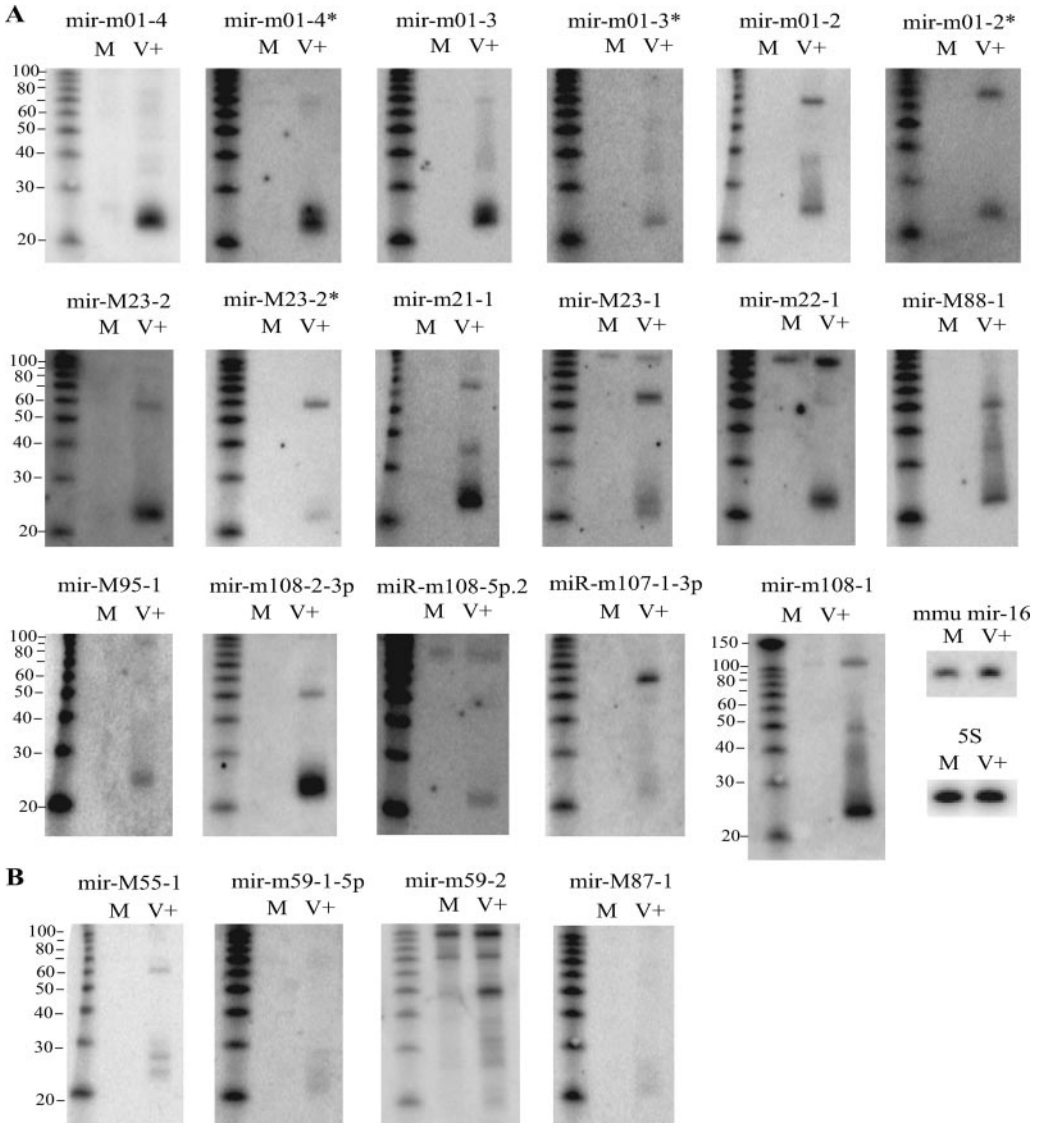

FIG. 2. Northern blots of MCMV miRNAs. RNA was extracted from NIH 3T3 cells 72 h after viral infection (V+). RNA from mock-infected cells (M) is included for comparison. Twenty micrograms of RNA was loaded onto each lane, and an RNA marker was included for size reference (the unlabeled, leftmost lane of each blot). Probes directed against mouse mir16 and 5S RNA were used as controls. The positions of molecular size markers (in nucleotides) are shown to the left of the blots. *Mus musculus* (mmu) mir-16 was also included in the analysis. (A) Blots of miRNAs validated in this report; (B) blots of RNAs cloned but not scored as miRNAs in this report.

some of the heterogeneity we observe by Northern blotting could be related to posttranscriptional modification of the miRNAs (S. Pfeffer, personal communication).

From the 17 mature miRNAs cloned and validated, 6 (derived from 4 distinct precursors) are represented in the top 10 predicted precursors in Table 1 (these are noted in bold type in Tables 1 and 2). Notably, two miRNAs were highly abundant in these cloning studies: mir-m01-3 represented 30% of viral clones and was present in the top 10 predicted precursors, and mir-m108-2-3p represented 20% of viral clones. On the basis of data sharing with S. Pfeffer (IBMP-CNRS) and discussion with S. Griffiths-Jones (University of Manchester), we agreed on a naming convention to reflect the genomic locations of the miRNAs and to facilitate comparison and standardization of our results. These names are as they will appear in the miRNA registry (15).

There are a few notable properties of the cloned miRNAs. Several sequences exhibited 3′ heterogeneity, as has been seen with many miRNAs previously (24, 36, 52), as well as nongenomic sequence at the 3′ end (23) (Table 2). mir-M23-2 is the only validated miRNA that exhibited significant 5′ heterogeneity; mir-M23-2 was cloned with two different 5′ start sites. Although this result could be indicative of a random degradation product, we include this as a validated miRNA because it is detected as an abundant, homogeneous product on a Northern blot (Fig. 2A) and is expected to originate from a precursor stem-loop structure, since mir-M23-2* was also cloned (and it is predicted in Table 1).

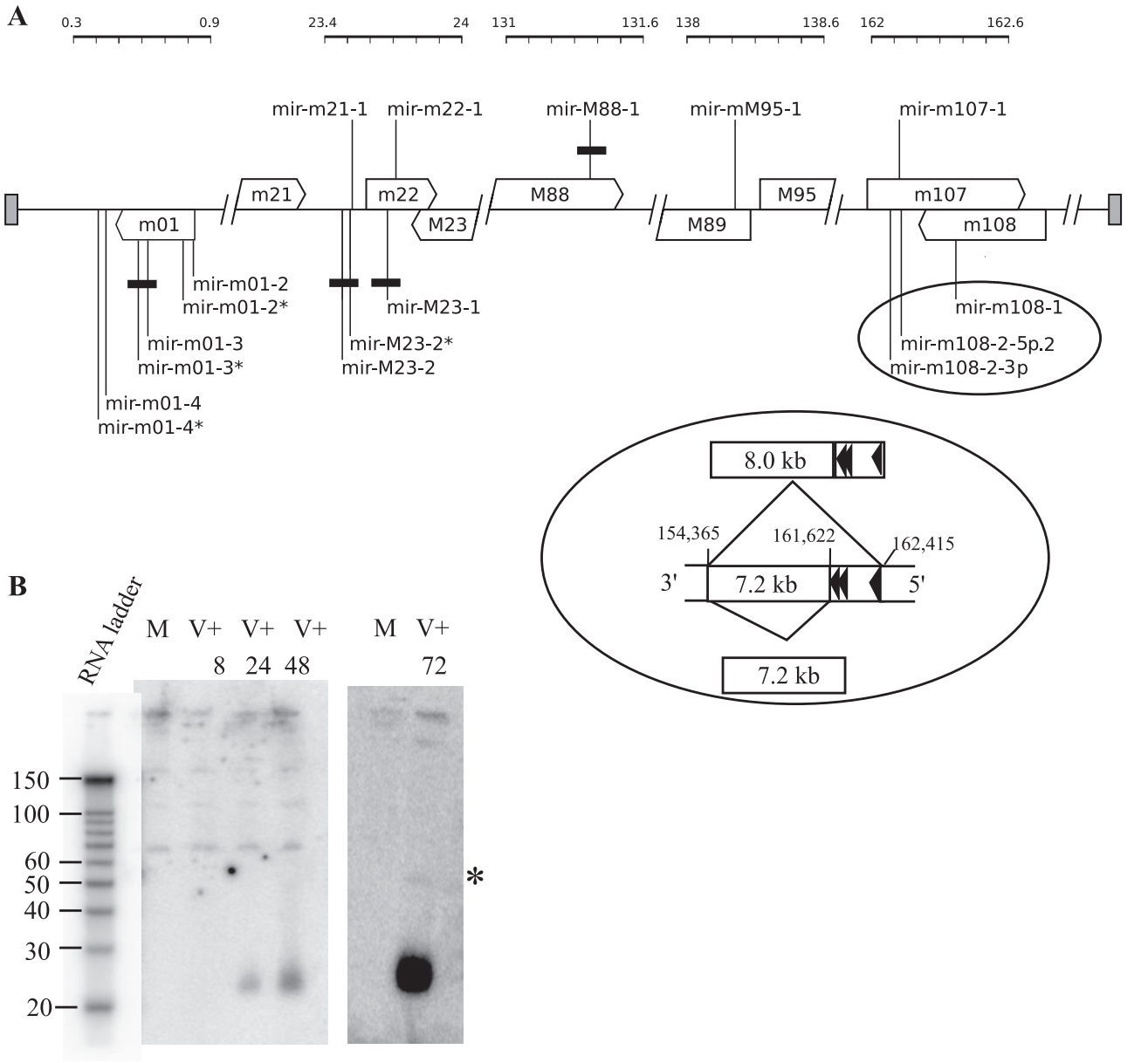

FIG. 3. Genomic organization of MCMV miRNAs. (A) Diagram depicting the regions of the MCMV genome that contain MCMV miRNAs. Rulers indicate the genomic position in kilobases; broken lines are used to indicate a break in the scale. The predicted open reading frames in the vicinity of the miRNAs are noted with open triangles and are above the genome line if they are on the sense strand and below the genome line if they are on the antisense strand (the same format is used for depicting the miRNAs). The black rectangles are the predicted miRNA precursors from Table 1, overlaid on the miRNAs cloned in this study. The oval inset depicts the spatial relationship (not to scale) between mir-m108-2-3p, mir-m108-2-5p.2, and mir-m108-1 (drawn as black triangles) and the two introns previously identified (depicted from 3′ to 5′, to be consistent with the diagram of the whole genome above); both the 5′ splice sites are noted as well as the 3′ splice site. (B) Northern blot of mir-m108-2-3p at the indicated time points (hours) after infection. Lanes: M, mock-infected cells; V+, virus-infected cells. The positions of molecular size markers (in nucleotides) are shown to the left of the blot. The asterisk indicates the faint precursor band near the 50-nt RNA marker.

Structure and organization of the microRNAs. There are a number of notable structural features of the cloned miRNAs. In particular, the miRNAs are organized into five genomic regions and three clusters (Fig. 3A). In the clusters defined in this study, miRNAs occur within 500 nt of one another, on either strand of the genome. We name clusters in this study according to the open reading frames (ORFs) in the proximity of the miRNAs. In the clusters around m21/m22/M23 and m107/m108, miRNAs exist in overlapping regions on complementary strands of the genome, which has not previously been observed with other viral miRNAs. According to the gene annotation system of Rawlinson and colleagues (41) (system adopted for Fig. 3A), 9 of the 17 miRNAs fall outside of the annotated regions (in predicted 3′ untranslated regions [3′UTRs] or 5′ to predicted ORFs), and 8 fall within annotated ORFs. Five miRNAs also lie opposite predicted ORFs. Within the cluster

near m01, two precursor miRNAs are within the ORF, while one precursor miRNA lies in the 3′UTR (Fig. 3A). Previous RT-PCR analysis detected m01 in NIH 3T3 cells using RT-PCR (50); however, the exact boundaries of the predicted ORF have not been experimentally verified. On the basis of the location of miRNAs near m22 and M23 (within or between ORFs), it is not obvious from which transcripts these miRNAs might be derived.

Of particular interest are three miRNAs, mir-m108-2-3p, mir-m108-2-5p.2, and mir-m108-1 that lie within and 3′ to m108 (41). A recent report by Kulesza and Shenk (21) demonstrated that MCMV encodes a 7.2-kb stable intron that occurs in this vicinity; a less abundant 8.0-kb intron was also reported (21), which would encompass the miRNAs in this cluster (Fig. 3A, inset). It is expected that these miRNAs could exist as either introns or exons, depending on splicing. The second most abundant miRNA (20% of viral clones), mir-m108-2-3p, is contained in this region, and the processed (~23-nt) miRNA is readily abundant on a Northern blot and displays a clear band consistent with a precursor sequence (Fig. 2A and 3B). Work is currently under way to determine the relationship between the miRNAs in this cluster and the 7.2-kb and 8.0-kb introns.

According to the stem-loop precursor sequences predicted for the MCMV miRNAs, the length of the 3′ overhangs between mature miRNAs ranges from 1 to 5 nt; these overhang lengths have also been seen previously with miRNAs from Kaposi's sarcoma-associated herpesvirus (36), HCMV (7) and Marek's disease virus (MDV) (52). Curiously, both mir-m108-2-3p and mir-m108-2-5p.2 could be derived from the same precursor but do not appear to originate from a classical intermediate, since they would require 5′ overhangs (rather than 3′ overhangs). We questioned whether this result might indicate that these RNAs are small interfering RNAs (siRNAs), rather than miRNAs (1), which would be consistent with RNAs being cloned from both strands of the genome in overlapping regions (Table 2). siRNAs come from long double-stranded RNA (dsRNA) molecules processed such that many small RNAs accumulate from both strands of the dsRNA; if this were the case, therefore, mir-m108-2-3p and mir-m108-2-5p.2 would be processed as siRNAs from a fully complementary dsRNA intermediate. This would require that both the antisense strand and the sense strand be transcribed. In support of this, we did detect a miRNA, mir-m107-1, on the sense strand that overlaps mir-m108-2-5p.2 (Fig. 3A). However, both mir-m108-2-3p and mir-m107-1 have distinct precursors that are detected on Northern blots (Fig. 2A), and a probe directed against the sequence between mir-m108-2-3p and mir-m108-2-5p.2 failed to detect any small RNAs on a Northern blot or by RT-PCR (data not shown). Also relevant is the fact that Dölken et al. (6a) cloned a different 5′ version of mir-m108-2, which forms a more classical miRNA intermediate with mir-m108-2-3p.

Detection in macrophage cells. Since macrophages are assumed to be a key cell type for in vivo infection, we performed RT-PCR to determine whether these MCMV miRNAs are expressed in both fibroblasts and macrophage cells. Although initial cloning studies with BMM cells showed a low level of viral content (see above), all of the validated MCMV miRNAs in Table 2 were readily detected in macrophage (BMM) and fibroblast (NIH 3T3) cells using RT-PCR, with the exception of miR-m108-1. The RT-PCR products were sized at the predicted length (~65 to 70 nt), based on detection of the mature miRNA with the poly(A) tail protocol described above. Gel analysis confirms that the products are specific to infected cells (Fig. 4).

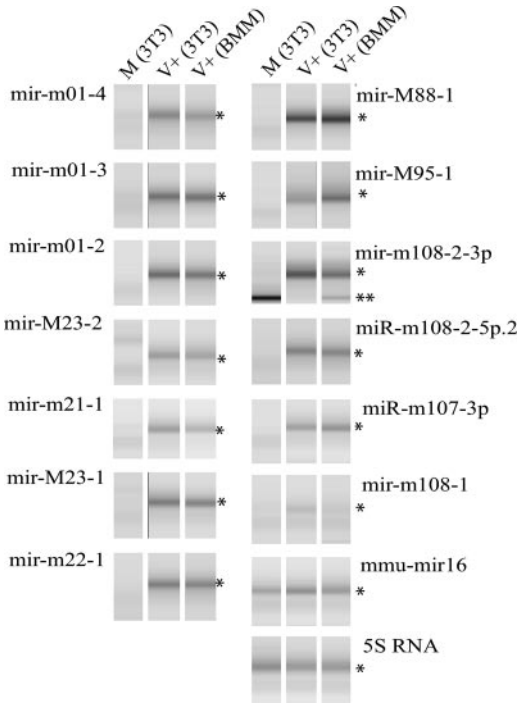

FIG. 4. Detection of MCMV miRNAs in bone marrow-derived macrophages. RNA was extracted from NIH 3T3 (3T3) or BMM cells 72 h after infection with MCMV (MOI of 1). RNA from mock-infected cells (M) and virus-infected (V+) cells was poly(A) tailed, reverse transcribed, and subjected to RT-PCR. The RT-PCR product (0.5 μl) was loaded on the Lab901 D800 ScreenTape, which automatically separated and sized the amplified products by gel electrophoresis and integrated software. The bands indicated with an asterisk were all sized between 64 and 70 nt, as expected from the RT-PCR protocol; additional bands (band with two asterisks) were observed for mir-m108-2-3p that corresponded to primer-dimer products with distinguishable dissociation curves.

Kinetic class analysis of MCMV miRNAs. Like other herpesviruses, the expression of genes in MCMV is organized into a cascade of immediate-early, early, and late transcription (32). The immediate-early genes are the first genes expressed upon infection and are strictly dependent on the host cell translational machinery. These genes are implicated in the evasion of host immune responses and the control of early and late transcripts of the virus. Early genes are, by definition, dependent on the immediate-early genes, while late genes are dependent on viral DNA replication. In order to determine the kinetic classes of each miRNA, viral infections were performed in the presence of cycloheximide (a block to immediate-early protein synthesis) or phosphonoacetic acid (an inhibitor of viral replication), and the relative amount of each miRNA was quantified. Quantification of miRNAs was performed using SYBR green RT-PCR which was optimized to ensure the specificity of detection for the mature miRNAs (Materials and Methods).

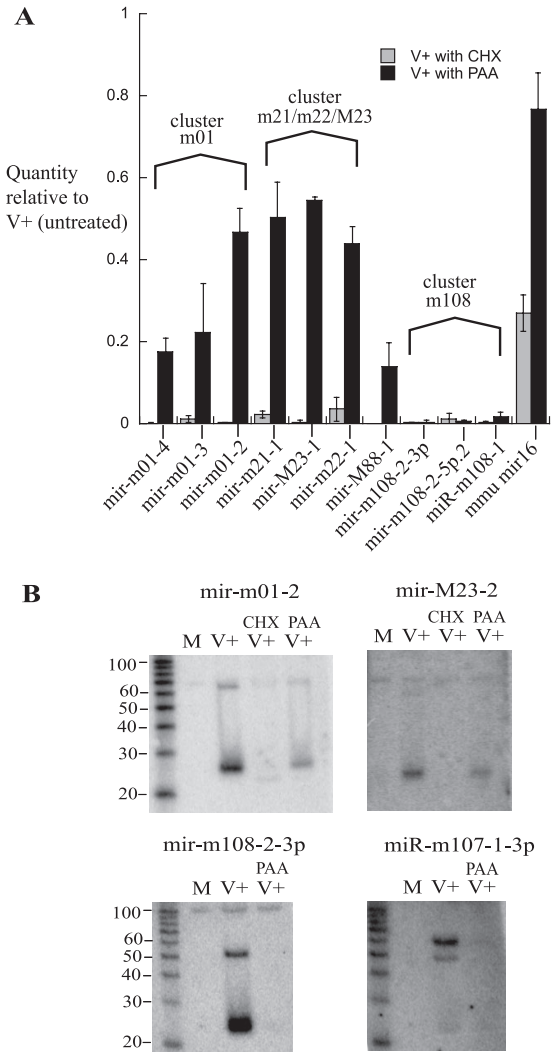

FIG. 5. Kinetic classes of MCMV miRNAs. (A) Relative values of each miRNA from RNA samples extracted from NIH 3T3 cells infected with MCMV (MOI of 2) in the presence or absence of cycloheximide (CHX) (100 μg/ml) or phosphonoacetic acid (PAA) (250 μg/ml) after 24 h. The RNA was from mock-infected cells (M) or virus-infected cells (V+). Data shown are the averages for two biological replicates (each of which was an average from three technical replicates); error bars represent the standard deviations. Data were normalized for each miRNA by setting the quantity of the miRNA in untreated, but infected, samples at 1.0. *Mus musculus* (mmu) mir-16 was also included in the analysis. (B) Northern blots of mir-m01-2 and mir-m108-2-3p (for validation of the qRT-PCR results) are shown on the left. Blots of mir-M23-2 and mir-m107-1-3p shown on the right are included for kinetic class characterization of these miRNAs. The positions of molecular size markers (in nucleotides) are shown to the left of the blots.

As shown in Fig. 5A, all MCMV miRNAs examined are sensitive to cycloheximide treatment and therefore require immediate-early proteins for their expression. mir-m108-2-3p, mir-m108-2-5p.2, and mir-m108-1 also show dependence on viral replication and, therefore, fall into the late kinetic class. The Northern blots in Fig. 5B demonstrate that mir-M23-2 is an early gene product and mir-m107-1-3p is a late gene product (these miRNAs were unsuitable for qRT-PCR analysis; Materials and Methods); however, based on the low signal observed for mir-m107-1-3p, it is difficult to accurately characterize this miRNA. Northern blots of mir-m01-2 and mir-m108-2-3p are provided (Fig. 5B) to compare and validate the qRT-PCR data in Fig. 5A. We also examined murine mir16 as a control under these conditions to ensure that the drugs used did not interfere with the biogenesis of the mature miRNAs (Fig. 5A). However, one assumption in using this control is that host and viral miRNAs utilize the same (host) protein factors for their biogenesis, which requires further characterization. Unlike other viral kinetic class analyses, we identified the presence of the mature miRNA product with qRT-PCR, not the transcript from which it is derived. It is possible, therefore, that the miRNA transcripts are produced in an earlier class but require other viral products for their biogenesis.

DISCUSSION

Since the discovery of miRNAs in EBV 3 years ago, research with viral miRNAs has greatly enhanced our knowledge of miRNA biogenesis and virus-host interactions (6, 44, 45). In the current study, we utilized a bioinformatic approach to examine the potential for precursor miRNA sequences in the MCMV genome. Although this study was not exhaustive, 6 of the cloned mature miRNAs (derived from 4 precursors) are contained within the top 10 predicted precursors; the accompanying report by Dölken et al. (6a) further validates 2 of the predicted precursors, as noted in Table 1. In summary, we have identified a total of 17 mature miRNAs from MCMV, adding to the list of roughly 100 known miRNAs from herpesviruses (15). In addition, we identified a highly abundant miRNA, mir-m108-2-3p (20% of viral clones) from a region of the genome that was not predicted to encode precursors in our computational analysis. The location of this miRNA, and the other miRNAs that cluster in this region, is particularly relevant because they are in the immediate vicinity of a previously identified stable intron and can in exist in two different forms, depending on splicing. Significantly, Shenk and colleagues showed that mutation of the splice sites for the 7.2-kb intron influences the progression from the acute phase to the persistent phase of infection in vivo; this mutation could also influence the form (exonic or intronic) in which mir-m108-2-3p, mir-m108-2-5p.2, and mir-m108-1 exist (Fig. 3A). Understanding the relationship between this phenotype and the regulation of the miRNAs is an important topic that requires further study. It is noteworthy that work with HSV demonstrated that a miRNA (mir-LAT1) is also positioned adjacent to a stable intron in the latency-associated transcript (LAT). It remains to be seen whether the spatial relationship between miRNAs and stable introns is a common feature in viruses and what role this plays in pathogenesis. However, the MCMV stable intron is orthologous to the HCMV stable intron (20, 39), and miRNAs have not previously been cloned in its vicinity.

In general, the lack of conservation between MCMV and HCMV miRNAs is consistent with the general lack of conservation among herpesvirus-encoded miRNAs (33, 36). One recent report demonstrated conservation of 7 out of 16 miRNAs in EBV and rhesus lymphocryptovirus (separated by ≥13 million years) (5); however, analysis of miRNAs in Marek's disease virus type 1 (MDV-1) and MDV-2 (estimated to be sep-

arated by ~26 million years) showed no sequence conservation (52). Although this lack of conservation could indicate a lack of functional significance, it also possible that a primary function of virus-encoded miRNAs is to target host genes, as has been demonstrated in HSV-1 and HCMV (cited above). The host 3′UTR target sites need not be conserved to be functionally relevant (8), and the viral miRNA sequences could be significantly influenced by coevolution with the host. This is particularly relevant in the case of herpesviruses, whose evolution has occurred on the same timescale as mammalian speciation (31). Ultimately, true understanding of herpesvirus miRNA function and evolution will require a global analysis of their targets, both host and viral. Potential host (mouse) targets of these MCMV miRNAs were examined using the miRANDA program (A. Enright, personal communication); however, each miRNA is predicted to target up to ~800 genes, and experimental validation is required to understand the relevance of these predictions.

A striking feature of the MCMV miRNAs is their localization on both strands of the genome in specific regions. In the cluster around m107/m108, for example, mir-m107-1-3p (on the sense strand) overlaps mir-m108-2-5p.2 on the antisense strand. Previously it was shown in SV40 that a miRNA targets a perfectly complementary mRNA that was encoded on the opposite strand of the genome. However, mir-m107-1-3p overlaps mir-m108-2-5p.2 by only 10 bp, and there is no precedence for miRNAs regulating one another in this fashion. The detection of distinct pre-miRNAs for mir-m108-2-3p and mir-m107-1-3p (Fig. 2 and Fig. 5B) argues against the possibility that they are siRNAs derived from a dsRNA intermediate. According to computational predictions, precursor miRNAs are predicted to occur on complementary strands of the genome in overlapping regions (Table 1). It may be that this is another way in which viruses have evolved to most efficiently utilize their genomes. Alternatively, there may be some evolutionary or regulatory factors that select for such a genomic organization.

An important result from this study is the identification of viral miRNAs clustered in close proximity (<500 nt) and on complementary strands of the genome within and around predicted ORFs. For example, miRNAs are clustered around m1 and m22, which have not been shown to encode proteins. These results imply that there are likely to be noncoding gene transcripts which are not accounted for in the current genomic maps based on annotation of ORFs and that the boundaries of the predicted ORFs at present do not accurately reflect the location of miRNA transcriptional activity. Relevant to this, a recent cDNA cloning study from HCMV-infected cells demonstrated that 45% of the clones were from regions of the genome that were predicted to be noncoding (53).

It is now widely recognized that CMV is not only capable of evading the immune response but it can also proactively induce immunosuppression in humans (34). Understanding the mechanisms by which CMV establishes an acute infection and persists in a latent state is, therefore, of clinical relevance. Although extensive work has been undertaken in the characterization of CMV open reading frames which are important for viral function and immune evasion, there is still a lack of understanding in the area of CMV-host interactions, which evades the development of effective therapeutics (9). A recent report with HCMV demonstrated that a 2.7-kb ncRNA interacts with components of the mitochondrial respiratory chain complex and thereby modulates cellular metabolic activity in order to enable a productive viral life cycle (42). Clearly, there are numerous potential mechanisms by which noncoding RNAs, including miRNAs, could influence viral infection and latency.

To conclude, we demonstrate by computational and cloning analyses that MCMV has the capacity to encode miRNAs clustered throughout the genome on complementary strands, including in the vicinity of the 7.2-kb stable intron. This work points to a variety of potential regulatory mechanisms for MCMV miRNAs, the study of which will undoubtedly expand the repertoire of virus-host interactions important for CMV infection and latency.

ACKNOWLEDGMENTS

This work was supported by the INFOBIOMED NoE FP6-IST-2002-507585 EU-funded project to P.G. and the Wellcome Trust (066784) to P.G. A.H.B. was supported by a Marie Curie Fellowship (EU) and a Thomas Work fellowship through the Center for Infectious Diseases at the University of Edinburgh. J.S.-L. was supported by eDIKT2.

We thank A. Hatzigeorgiou and A. Oulas for advice on bioinformatic predictions; A. Enright and C. Abreu-Goodger for helpful discussions regarding target predictions; and D. Page, G. Sing, and other members of the Division of Pathway Medicine for helpful discussions. We also thank L. Dölken and S. Pfeffer for sharing unpublished observations while we were preparing the manuscript and Lab901 for allowing us to use their automated ScreenTape platform for analysis of RT-PCR products.

REFERENCES

1. **Ambros, V., B. Bartel, D. P. Bartel, C. B. Burge, J. C. Carrington, X. Chen, G. Dreyfuss, S. R. Eddy, S. Griffiths-Jones, M. Marshall, M. Matzke, G. Ruvkun, and T. Tuschl.** 2003. A uniform system for microRNA annotation. RNA **9:**277–279.
2. **Angulo, A., P. Ghazal, and M. Messerle.** 2000. The major immediate-early gene *ie3* of mouse cytomegalovirus is essential for viral growth. J. Virol. **74:**11129–11136.
3. **Bennasser, Y., S. Y. Le, M. L. Yeung, and K. T. Jeang.** 2006. MicroRNAs in human immunodeficiency virus-1 infection. Methods Mol. Biol. **342:**241–253.
4. **Bonnet, E., J. Wuyts, P. Rouze, and Y. Van de Peer.** 2004. Evidence that microRNA precursors, unlike other non-coding RNAs, have lower folding free energies than random sequences. Bioinformatics **20:**2911–2917.
5. **Cai, X., A. Schafer, S. Lu, J. P. Bilello, R. C. Desrosiers, R. Edwards, N. Raab-Traub, and B. R. Cullen.** 2006. Epstein-Barr virus microRNAs are evolutionarily conserved and differentially expressed. PLoS Pathog. **2:**e23.
6. **Cullen, B. R.** 2006. Viruses and microRNAs. Nat. Genet. **38**(Suppl.)**:**S25–S30.

6a. **Dölken, L., J. Perot, V. Cognat, A. Alioua, M. John, J. Soutschek, Z. Ruzsics, U. Koszinowski, O. Voinnet, and S. Pfeffer.** 2007. Mouse cytomegalovirus microRNAs dominate the cellular small RNA profile during lytic infection and show features of posttranscriptional regulation. J. Virol. **81:**13771–13782.

7. **Dunn, W., P. Trang, Q. Zhong, E. Yang, C. van Belle, and F. Liu.** 2005. Human cytomegalovirus expresses novel microRNAs during productive viral infection. Cell. Microbiol. **7:**1684–1695.
8. **Farh, K. K., A. Grimson, C. Jan, B. P. Lewis, W. K. Johnston, L. P. Lim, C. B. Burge, and D. P. Bartel.** 2005. The widespread impact of mammalian microRNAs on mRNA repression and evolution. Science **310:**1817–1821.
9. **Fruh, K., K. Simmen, B. G. Luukkonen, Y. C. Bell, and P. Ghazal.** 2001. Virogenomics: a novel approach to antiviral drug discovery. Drug Discov. Today **6:**621–627.
10. **Furnari, F. B., M. D. Adams, and J. S. Pagano.** 1993. Unconventional processing of the 3′ termini of the Epstein-Barr virus DNA polymerase mRNA. Proc. Natl. Acad. Sci. USA **90:**378–382.
11. **Ghazal, P., M. Messerle, K. Osborn, and A. Angulo.** 2003. An essential role of the enhancer for murine cytomegalovirus in vivo growth and pathogenesis. J. Virol. **77:**3217–3228.
12. **Ghazal, P., A. E. Visser, M. Gustems, R. Garcia, E. M. Borst, K. Sullivan, M. Messerle, and A. Angulo.** 2005. Elimination of *ie*1 significantly attenuates murine cytomegalovirus virulence but does not alter replicative capacity in cell culture. J. Virol. **79:**7182–7194.

13. **Grey, F., A. Antoniewicz, E. Allen, J. Saugstad, A. McShea, J. C. Carrington, and J. Nelson.** 2005. Identification and characterization of human cytomegalovirus-encoded microRNAs. J. Virol. **79:**12095–12099.
14. **Griffiths, P. D., and S. Walter.** 2005. Cytomegalovirus. Curr. Opin. Infect. Dis. **218:**241–245.
15. **Griffiths-Jones, S.** 2006. miRBase: the microRNA sequence database. Methods Mol. Biol. **342:**129–138.
16. **Gupta, A., J. J. Gartner, P. Sethupathy, A. G. Hatzigeorgiou, and N. W. Fraser.** 2006. Anti-apoptotic function of a microRNA encoded by the HSV-1 latency-associated transcript. Nature **442:**82–85.
17. **Hofacker, I. L.** 2003. Vienna RNA secondary structure server. Nucleic Acids Res. **31:**3429–3431.
18. **Jopling, C. L., M. Yi, A. M. Lancaster, S. M. Lemon, and P. Sarnow.** 2005. Modulation of hepatitis C virus RNA abundance by a liver-specific microRNA. Science **309:**1577–1581.
19. **Krmpotic, A., I. Bubic, B. Polic, P. Lucin, and S. Jonjic.** 2003. Pathogenesis of murine cytomegalovirus infection. Microbes Infect. **5:**1263–1277.
20. **Kulesza, C. A., and T. Shenk.** 2004. Human cytomegalovirus 5-kilobase immediate-early RNA is a stable intron. J. Virol. **78:**13182–13189.
21. **Kulesza, C. A., and T. Shenk.** 2006. Murine cytomegalovirus encodes a stable intron that facilitates persistent replication in the mouse. Proc. Natl. Acad. Sci. USA **103:**18302–18307.
22. **Lagos-Quintana, M., R. Rauhut, W. Lendeckel, and T. Tuschl.** 2001. Identification of novel genes coding for small expressed RNAs. Science **294:**853–858.
23. **Landgraf, P., M. Rusu, R. Sheridan, A. Sewer, N. Iovino, A. Aravin, S. Pfeffer, A. Rice, A. O. Kamphorst, M. Landthaler, C. Lin, N. D. Socci, L. Hermida, V. Fulci, S. Chiaretti, R. Foa, J. Schliwka, U. Fuchs, A. Novosel, R. U. Muller, B. Schermer, U. Bissels, J. Inman, Q. Phan, M. Chien, D. B. Weir, R. Choksi, G. De Vita, D. Frezzetti, H. I. Trompeter, V. Hornung, G. Teng, G. Hartmann, M. Palkovits, R. Di Lauro, P. Wernet, G. Macino, C. E. Rogler, J. W. Nagle, J. Ju, F. N. Papavasiliou, T. Benzing, P. Lichter, W. Tam, M. J. Brownstein, A. Bosio, A. Borkhardt, J. J. Russo, C. Sander, M. Zavolan, and T. Tuschl.** 2007. A mammalian microRNA expression atlas based on small RNA library sequencing. Cell **129:**1401–1414.
24. **Lau, N. C., L. P. Lim, E. G. Weinstein, and D. P. Bartel.** 2001. An abundant class of tiny RNAs with probable regulatory roles in Caenorhabditis elegans. Science **294:**858–862.
25. **Lecellier, C. H., P. Dunoyer, K. Arar, J. Lehmann-Che, S. Eyquem, C. Himber, A. Saib, and O. Voinnet.** 2005. A cellular microRNA mediates antiviral defense in human cells. Science **308:**557–560.
26. **Lee, R. C., and V. Ambros.** 2001. An extensive class of small RNAs in Caenorhabditis elegans. Science **294:**862–864.
27. **Lee, Y., M. Kim, J. Han, K. H. Yeom, S. Lee, S. H. Baek, and V. N. Kim.** 2004. MicroRNA genes are transcribed by RNA polymerase II. EMBO J. **23:**4051–4060.
28. **Lewis, B. P., C. B. Burge, and D. P. Bartel.** 2005. Conserved seed pairing, often flanked by adenosines, indicates that thousands of human genes are microRNA targets. Cell **120:**15–20.
29. **Li, S. C., C. K. Shiau, and W. C. Lin.** 28 August 2007, posting date. Vir-Mir db: prediction of viral microRNA candidate hairpins. Nucleic Acids Res. doi:10.1093/nar/gkm610.
30. **Mathews, M. B., and T. Shenk.** 1991. Adenovirus virus-associated RNA and translation control. J. Virol. **65:**5657–5662.
31. **McGeoch, D. J., S. Cook, A. Dolan, F. E. Jamieson, and E. A. Telford.** 1995. Molecular phylogeny and evolutionary timescale for the family of mammalian herpesviruses. J. Mol. Biol. **247:**443–458.
32. **Mocarski, E. S.** 1996. Cytomegaloviruses and their replication. Lippincott-Raven Publishers, Philadelphia, PA.
33. **Nair, V., and M. Zavolan.** 2006. Virus-encoded microRNAs: novel regulators of gene expression. Trends Microbiol. **14:**169–175.
34. **Naniche, D., and M. B. Oldstone.** 2000. Generalized immunosuppression: how viruses undermine the immune response. Cell. Mol. Life Sci. **57:**1399–1407.
35. **Omoto, S., and Y. R. Fujii.** 2006. Cloning and detection of HIV-1-encoded microRNA. Methods Mol. Biol. **342:**255–265.
36. **Pfeffer, S., A. Sewer, M. Lagos-Quintana, R. Sheridan, C. Sander, F. A. Grasser, L. F. van Dyk, C. K. Ho, S. Shuman, M. Chien, J. J. Russo, J. Ju, G. Randall, B. D. Lindenbach, C. M. Rice, V. Simon, D. D. Ho, M. Zavolan, and T. Tuschl.** 2005. Identification of microRNAs of the herpesvirus family. Nat. Methods. **2:**269–276.
37. **Pfeffer, S., and O. Voinnet.** 2006. Viruses, microRNAs and cancer. Oncogene **25:**6211–6219.
38. **Pfeffer, S., M. Zavolan, F. A. Grasser, M. Chien, J. J. Russo, J. Ju, B. John, A. J. Enright, D. Marks, C. Sander, and T. Tuschl.** 2004. Identification of virus-encoded microRNAs. Science **304:**734–736.
39. **Plachter, B., B. Traupe, J. Albrecht, and G. Jahn.** 1988. Abundant 5 kb RNA of human cytomegalovirus without a major translational reading frame. J. Gen. Virol. **69:**2251–2266.
40. **Platt, J.** 2000. Probabilistic outputs for support vector machines and comparison to regularized likelihood methods, p. 61–74. *In* P. J. Bartlett, B. Schölkop, D. Schuurmans, and A. J. Smola (ed.), Advances in large margin classifiers. The MIT Press, Cambridge, MA.
41. **Rawlinson, W. D., H. E. Farrell, and B. G. Barrell.** 1996. Analysis of the complete DNA sequence of murine cytomegalovirus. J. Virol. **70:**8833–8849.
42. **Reeves, M. B., A. A. Davies, B. P. McSharry, G. W. Wilkinson, and J. H. Sinclair.** 2007. Complex I binding by a virally encoded RNA regulates mitochondria-induced cell death. Science **316:**1345–1348.
43. **Sano, M., Y. Kato, and K. Taira.** 2006. Sequence-specific interference by small RNAs derived from adenovirus VAI RNA. FEBS Lett. **580:**1553–1564.
44. **Sarnow, P., C. L. Jopling, K. L. Norman, S. Schutz, and K. A. Wehner.** 2006. MicroRNAs: expression, avoidance and subversion by vertebrate viruses. Nat. Rev. Microbiol. **4:**651–659.
45. **Scaria, V., M. Hariharan, S. Maiti, B. Pillai, and S. K. Brahmachari.** 2006. Host-virus interaction: a new role for microRNAs. Retrovirology **3:**68.
46. **Shi, R., and V. L. Chiang.** 2005. Facile means for quantifying microRNA expression by real-time PCR. BioTechniques **39:**519–525.
47. **Stern-Ginossar, N., N. Elefant, A. Zimmermann, D. G. Wolf, N. Saleh, M. Biton, E. Horwitz, Z. Prokocimer, M. Prichard, G. Hahn, D. Goldman-Wohl, C. Greenfield, S. Yagel, H. Hengel, Y. Altuvia, H. Margalit, and O. Mandelboim.** 2007. Host immune system gene targeting by a viral miRNA. Science **317:**376–381.
48. **Sullivan, C. S., and D. Ganem.** 2005. MicroRNAs and viral infection. Mol. Cell **20:**3–7.
49. **Sullivan, C. S., A. T. Grundhoff, S. Tevethia, J. M. Pipas, and D. Ganem.** 2005. SV40-encoded microRNAs regulate viral gene expression and reduce susceptibility to cytotoxic T cells. Nature **435:**682–686.
50. **Tang, Q., E. A. Murphy, and G. G. Maul.** 2006. Experimental confirmation of global murine cytomegalovirus open reading frames by transcriptional detection and partial characterization of newly described gene products. J. Virol. **80:**6873–6882.
51. **Valoczi, A., C. Hornyik, N. Varga, J. Burgyan, S. Kauppinen, and Z. Havelda.** 2004. Sensitive and specific detection of microRNAs by Northern blot analysis using LNA-modified oligonucleotide probes. Nucleic Acids Res. **32:**e175.
52. **Yao, Y., Y. Zhao, H. Xu, L. P. Smith, C. H. Lawrie, A. Sewer, M. Zavolan, and V. Nair.** 2007. Marek's disease virus type 2 (MDV-2)-encoded microRNAs show no sequence conservation to those encoded by MDV-1. J. Virol. **81:**7164–7170.
53. **Zhang, G., B. Raghavan, M. Kotur, J. Cheatham, D. Sedmak, C. Cook, J. Waldman, and J. Trgovcich.** 2007. Antisense transcription in the human cytomegalovirus transcriptome. J. Virol. **81:**11267–11281.